Hydrogenation of CO 2 by a Bifunctional PC(sp 3)P Iridium(III) Pincer Complex Equipped with Tertiary Amine as a Functional Group

Stanislav Gelman-Tropp, Evgueni Kirillov, Evamarie Hey-Hawkins, Dmitri Gelman

10.1002/chem.202301915

Hydrogenation of CO_2 by a Bifunctional PC(sp^3)P Iridium(III) Pincer Complex Equipped with Tertiary Amine as a Functional Group

Stanislav Gelman-Tropp[a], Evgueni Kirillov,[b] Evamarie Hey-Hawkins[c]* and Dmitri Gelman[a]**

[a]Institute of Chemistry, The Hebrew University, Edmond Safra Campus, Givat Ram, 91904 Jerusalem, Israel. Fax: (+) 972-2-6585279. [b]Université de Rennes, CNRS, Institut des Sciences Chimiques de Rennes (ISCR), UMR 6226, F-35042 Rennes, France. E-mail: evgueni.kirillov@univ-rennes.fr; [c]Faculty of Chemistry and Mineralogy, Institute of Inorganic Chemistry, Leipzig University, Johannisallee 29, D-04103 Leipzig, Germany. E-mail: hey@uni-leipzig.de.

10.1002/chem.202301915

ABSTRACT

Reversible hydrogen storage in the form of stable and mostly harmless chemical substances such as formic acid (FA) is a cornerstone of a fossil fuels-free economy. In the past, we have reported a primary amine-functionalized bifunctional iridium(III)-PC(sp^3)P pincer complex as a mild and chemoselective catalyst for the additive-free decomposition of neat formic acid. In this manuscript, we report on the successful application of a redesigned complex bearing tertiary amine functionality as a catalyst for mild hydrogenation of CO_2 to formic acid. The catalyst demonstrates TON up to $6 \cdot 10^4$ and TOF up to $1.7 \cdot 10^4$ h^{-1}. In addition to the practical value of the catalyst, experimental and computational mechanistic studies provide the rationale for the design of improved next-generation catalysts.

KEYWORDS. ligand-metal cooperation, hydrogenation, CO_2, formic acid, pincer complexes.

Introduction

Continuous growth in the utilization of fossil fuels as the primary energy source puts much stress on the environment through the accumulation of carbon dioxide in the atmosphere and, consequently, the climate change caused by the greenhouse effect.[1] One of the most reasonable solutions to these global problems is the selective capture of CO_2 from industrial emissions, followed by its cost-efficient conversion to valuable products, including C1-building blocks for chemical transformations.[2] For example, the direct transformation of carbon dioxide to carbonates,[3] polycarbonates,[4] urea[5], and salicylic acid[6] is well established. On the other hand, its selective catalytic reduction to CO, methanol, formaldehyde, alkyl formates, and formic acid (FA) on an industrial scale is currently under intensive development.[7] In particular, hydrogenation of CO_2 to FA has become a key technological target because this non-toxic and non-corrosive bulk reagent for textile, construction, dye, and leather industries is mainly manufactured biotechnologically[8] or by hydrolysis of methyl formate, the methanol carbonylation product.[9]

Many earth-abundant[10] and noble metal-based[11] compounds have been studied as catalysts for CO_2 hydrogenation. Still, satisfactory catalyst performance and product selectivity remain an issue because carbon dioxide is an intrinsically stable molecule, lacking reactivity toward transition metals. Its inherent stability is due to the highly localized HOMO and LUMO orbitals - CO_2 is a moderate electron acceptor and a comparatively poor electron donor.[12] On the other hand, the formation of metal-carboxylate intermediates is associated with a significant energy change between the linear CO_2 and the bent carboxylate species.[13]

Nature overcomes this obstacle by creating multifunctional catalytic systems, for example, in Mo-Cu- or Ni-Fe-based CO dehydrogenases (CODH). The product selectivity and efficient CO_2 fixation are controlled by hydrogen bond-induced stabilization from neighboring histidine residues

10.1002/chem.202301915

located in a secondary coordination sphere of the enzymes.[14] Mimicking this bifunctional reactivity, small-molecule transition metal catalysts possessing secondary auxiliaries were designed and tested (Figure 1).[11l, 15]

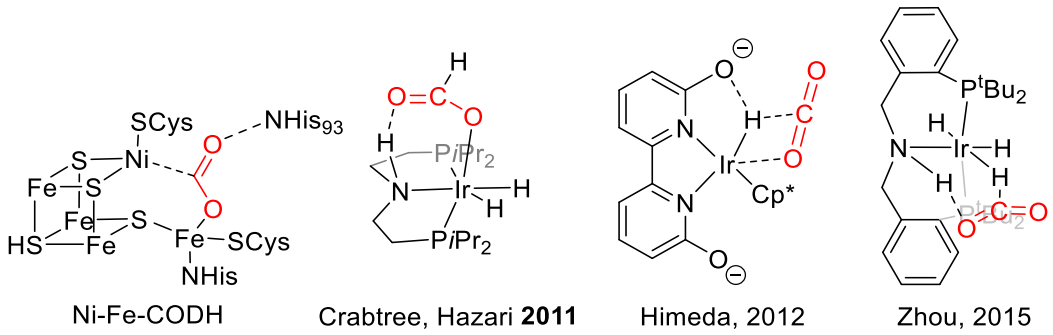

Figure 1. Examples of CO_2 stabilization by secondary interactions in the ligand scaffold.

Our group also demonstrated secondary effects in some bifunctional pincer complexes equipped with a functional pendant moiety.[16] In the context of the current topic, we found that the Ir-catalyzed dehydrogenation of formic acid to CO_2 and H_2 is considerably enhanced by the amine moiety in the secondary coordination sphere of complex **1** (Scheme 1, left). The catalyst (**1**), however, was found less reactive in a reversed process of hydrogenation of carbon dioxide.[17]

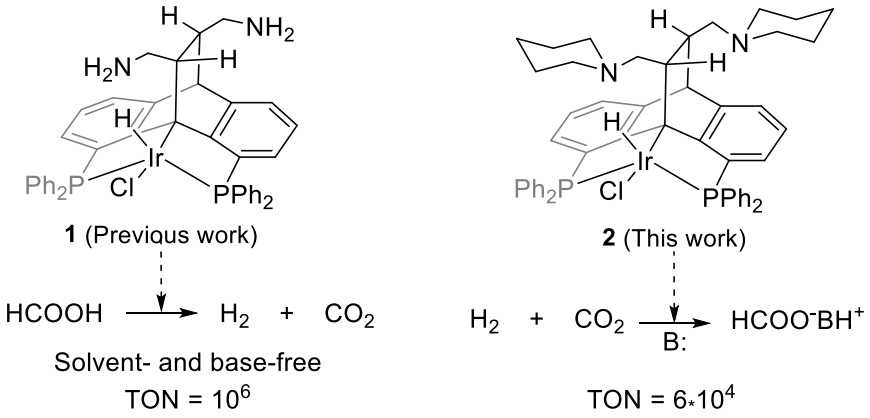

Scheme 1. Previously reported and new bifunctional catalysts.

In this manuscript, we report on a redesigned iridium(III)-PC(sp^3)P complex equipped with a tertiary amine moiety (**2**) as an efficient catalyst for the hydrogenation of CO_2 to FA (Scheme 1, right). We envisioned a dual effect of the sidearm in the secondary coordination sphere in **2**. First, we anticipated accelerating the heterolytic hydrogen activation process via intramolecular deprotonation of the pre-coordinated H_2 molecule by a more basic tertiary amine.[18] Second, we expected a more efficient CO_2 fixation[19] owing to the less coordinating nature of the amine with bulkier substituents.

Results and Discussion

Synthesis. The desired complex **2** was synthesized in three steps (Scheme 2). In the first step, a straightforward [2+4] cycloaddition between the bis-1,8-(diphenylphosphino)anthracene and (*E*)-1,4-di-1-piperidinyl-2-butene-1,4-dione as a dienophile afforded the corresponding Diels-Alder adduct **3** in 66% yield.[20] The bis-amide was subsequently reduced using $LiAlH_4$ to the desired pincer ligand **4** in 77% yield. The $^{31}P[^1H]$-NMR spectrum of the product showed characteristic doublets at δ = -17.7 and -19.9 ppm with through-space coupling ($J_{P,P}$ = 16.2 Hz) stressing desymmetrization of the phosphine donors (see SI for the crystallographic and spectral data).[21]

10.1002/chem.202301915

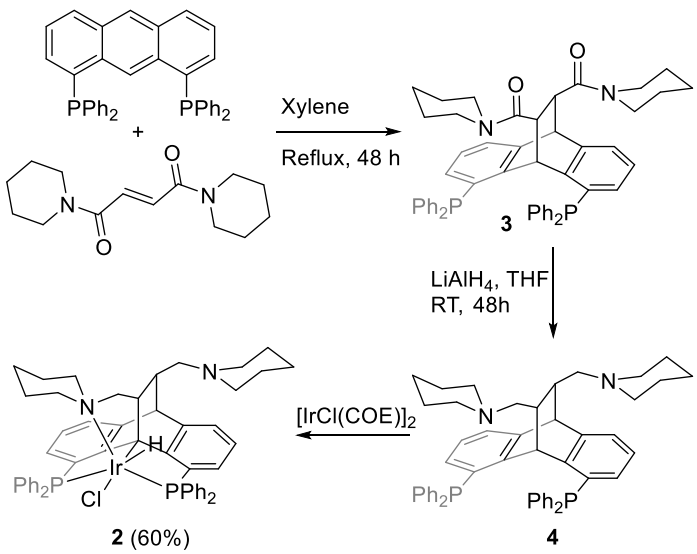

Scheme 2. Synthesis of complex **2**.

Finally, ligand **4** was successfully metalated using $[IrCl(COE)_2]_2$ (COE = cyclooctene) to provide the desired pincer complex **2** as a white powder in 60% yield.[22] As expected, the resulting $^{31}P[^{1}H]$-NMR signals were shifted downfield compared to the free ligand and appeared as a set of doublets at δ = 14.9 and 4.7 ppm with $J_{P2,H}$ = 25.7 Hz and $J_{P1,H}$ = 150.4 Hz. The corresponding ^{1}H-NMR spectrum displayed the hydride peak as a doublet of doublets at δ = -9.9 ppm ($J_{H,P2}$ = 32 Hz, $J_{H,P1}$ = 154.2 Hz). The significant difference between the $J_{P1,H}$ and $J_{P2,H}$ coupling constants suggests asymmetry of the hydride position with respect to the phosphine groups (i.e., *cis* and *trans*). Indeed, X-ray crystallographic analysis of a single crystal obtained from toluene clarified the connectivity in **2**. As can be seen in Figure 2, the iridium center is slightly distorted from an octahedral geometry with a chloride ligand located in a *trans* position to the metalated carbon atom. On the other hand, the *cisoid* hydride and the coordinated amine functional arm complement the octahedral base along with the *cisoid* phosphines. This arrangement of the hydride explains the observed P-H coupling.

10.1002/chem.202301915

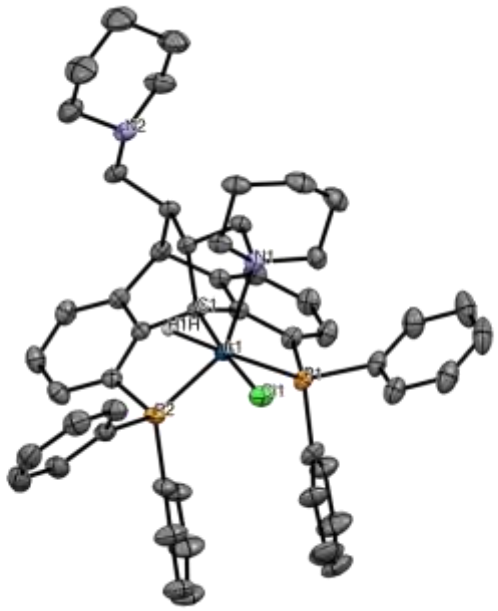

Figure 2. ORTEP drawing of complex **2** with the ellipsoids at 50% probability. Hydrogen atoms and solvent molecules are omitted for clarity. Selected bond lengths [Å] and angles [deg]: Ir-P1 2.353(7), Ir-P2 2.22(4), Ir-Cl 2.48(3), Ir-N 2.27(5), Ir-C1 2.04(2); P1-Ir-Cl 95.2(3), P2-Ir-Cl 98.6(6), P2-Ir-P1 105.2(8), P2-Ir-N1 151.7(3), N1-Ir-Cl1 93.4(3), N1-Ir-P1 98.3(3), C1-Ir-Cl 175.3(5), C1-Ir-P1 84.6(6), C1-Ir-P2 85.8(2), C1-Ir-N1 81.9(9), P2-Ir-H1 73.5(5), P1-Ir-H1 172.6(0).

Noteworthy, the mutual disposition of the phosphine and the hydride ligands remains stable also in non-coordinating solvents (e.g., toluene-d_8). On the other hand, new isomers formed in coordinating solvents such as acetonitrile or DMSO suggest facile dissociation of the pendant amine. The dissociation was probed using a TOCSY NMR technique showing no correlation between the hydride signal and the signals assigned to the aliphatic protons of the piperidine sidearm in THF or DMSO (SI, Figures S21 – S24).

Catalytic Studies. Table 1 summarizes representative optimization results (the complete table is provided in the SI, Table S1). Initially, the catalytic hydrogenation of CO_2 using 0.2 mol% of catalyst **2** was examined under base-free conditions using 40 atm of CO_2 and H_2 (1:3) at 130 °C

for 24 h in THF as a solvent. As expected, this nearly thermodynamically neutral process resulted in poor product yield. Therefore, further optimization experiments included the addition of a base as a limiting reagent, while the catalytic activity was represented by the formate yield based on its initial molar amount. The thermodynamic effect of a base on the hydrogenation of CO_2 to FA is well established: in its presence, the free energy of the transformation drops to a negative level.[23]

Thus, in a short series of experiments employing different organic bases (e.g., 1,8-diazabicyclo[5.4.0]undec-7-ene (DBU), 1,5-diazabicyclo[4.3.0]non-5-ene (DBN), triethylamine and diisopropylethylamine), the non-coordinating DBU was identified as the most suitable base to produce its formate salt leading to a 20% yield with a TON of 97, as shown in Table 1 (entries 1-4).[24] It is important to note that as DBU can transform CO_2 into a $DBUH^+$ bicarbonate adduct in the presence of water, dry DBU must be used for consistent results.[25]

Further optimization included solvent screening (Table 1, entries 4-8) which revealed that solvent polarity and nature play a significant role in the reaction, apparently, due to the solvation of the formate salt and a better solubility of the gas phase reactants (*i.e.,* CO_2 and H_2).[26] For example, while no conversion was observed in toluene, more polar acetonitrile or methanol drove the hydrogenation to completion under the initial conditions. Moreover, in protic methanol, high conversion was achieved after only one hour and even when the catalyst loading was reduced to 0.02 mol% with respect to DBU (TON = 4,550).

Table 1. Representative optimization results.

Entry	Cat. (mol%)	Time (h)	Temp. (°C)	P (CO_2:H_2 bar)	Solv.	Base	Conv. (%) [a]	TON [b]
1	0.2	24	130	10:30	THF	NEt(*i*Pr$_2$)	0	0
2	0.2	24	130	10:30	THF	NEt_3	0	0
3	0.2	24	130	10:30	THF	DBN	5	25

10.1002/chem.202301915

4	0.2	24	130	10:30	THF	DBU	19	97
5	0.2	24	130	10:30	Toluene	DBU	0	0
6	0.2	24	130	10:30	MeCN	DBU	99	500
7	0.2	1	130	10:30	MeOH	DBU	99	500
8	0.02	1	130	10:30	MeOH	DBU	90	4,550
9	0.02	1	110	10:40	MeOH	DBU	63	3,140
10	0.02	1	110	15:35	MeOH	DBU	86	4,315
11	0.02	1	110	20:30	MeOH	DBU	93	4,630
12	0.02	1	110	25:25	MeOH	DBU	90	4,500
13	0.02	1	110	30:20	MeOH	DBU	51	2,535
14	0.001	72	110	20:30	MeOH	DBU	60	60,500

[a] Conversion was calculated via NMR spectroscopic analysis with DMF as a standard, while the catalytic activity was represented by the formate yield based on its initial molar amount of DBU. [b] Turnover number is calculated as mol(substrate)/mol(catalysts). [c] Conversion to methyl formate under prolonged reaction time.

Even after lowering the reaction temperature, reasonable conversions were still reached; however, slightly higher pressure compensated for the milder heating. Remarkably, the catalyst performance showed a clear dependence on the partial pressure of CO_2. At the constant total pressure of 50 atm, the conversion constantly increased with increasing the CO_2 pressure from 10 to 20 atm and decreased after this point. Thus, the optimal reactivity of **2** was achieved under 50 atm of H_2/CO_2 (2:3), a temperature as low as 110 ºC in the presence of DBU as a base and in methanol as a solvent demonstrating the highest turnover number of 60,500 and conversion of 60% after 72 h (0.001 mol% of **2**). The initial turnover frequency of 17,170 h^{-1} was extracted from the first 10 minutes of the reaction (SI, Chart S1).[27] This performance is impressive if compared to the state-of-the-art catalysts under similar reaction conditions (*i.e.*, 100-120 ºC, 30-40 atm of CO_2/H_2, DBU as a base),[28] although Pidko's catalyst exhibits the highest activity under the similar conditions with TOF of 10^6 h^{-1}.[29]

10.1002/chem.202301915

Mechanistic Studies and DFT Calculations. The mechanistic hypothesis explaining these catalytic results is based on our previous studies on three-dimensional functionalized pincer complexes that revealed the participation of an appended functionality in the reversible activation/formation of chemical bonds. In particular, in the highly efficient dehydrogenation of FA catalyzed by the prototypical complex **1** under base-free conditions, both the experiment and DFT calculations suggested that protonated amino groups in the metal-formate intermediate induce stabilizing polar interactions, thus accelerating the decarboxylation step (Scheme 3).[17a]

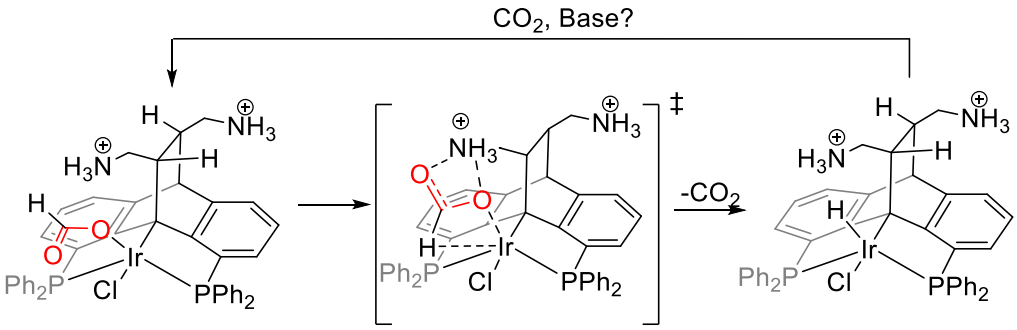

Scheme 3. Sidearm-assisted dehydrogenation of FA catalyzed by the prototypical **1**.

We also found that under base-free conditions, hydrogen liberation occurs via the non-oxidative protonolysis of the Ir−H bond and is mediated with the aid of the protonated amine sidearm leading to the formation of a cationic complex **1'** (Scheme 4).[17a]

10.1002/chem.202301915

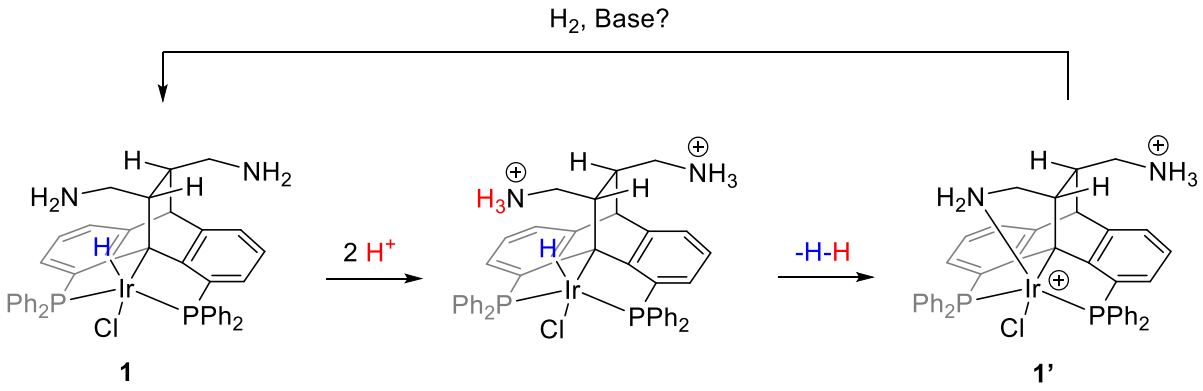

Scheme 4. Sidearm-assisted hydrogen formation in the prototypical **1**.

Based on these observations, the hydrogenation mechanism by pre-catalyst **2** could involve the intermediacy of structurally related species, although some corrections related to the presence of a base should be made.

With respect to the hydride transfer step, we considered three alternatives. The first involves a direct CO_2 insertion into the Ir–H bond of the protonated **2H**$^+$ to form the Ir-formate species (pathway A, Scheme 5). This pathway may arguably be facilitated by stabilizing a negatively charged transition state via interaction with the positively charged ammonium sidearm, as was established for the prototypical FA dehydrogenation catalyst **1** (Scheme 2). Alternatively, deprotonation of **2H**$^+$ to **2** by excess base (DBU) allows direct hydrogen transfer to the precoordinated carbon dioxide (pathway B, Scheme 5). Finally, nucleophilic pre-activation of the inherently stable CO_2 molecule via forming a covalent carbamate-like intermediate with the pendant amine before the hydride transfer may be considered (pathway C, Scheme 5).[30] This mode of CO_2 fixation mimics an active site of photosynthetic ribulose-1,5-bisphosphate carboxylase oxygenase enzyme, which reversibly binds CO_2 via N-C bond formation (carbamate intermediate) with a lysine residue in the secondary coordination sphere.[31]

10.1002/chem.202301915

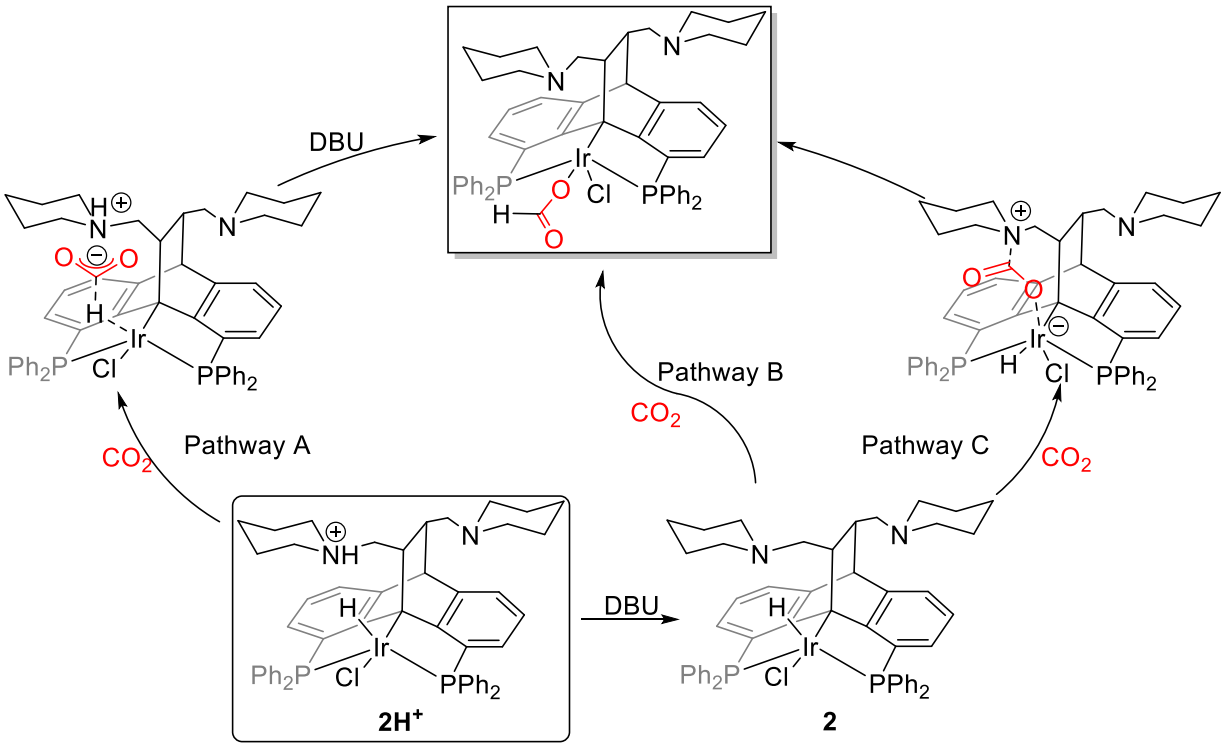

Scheme 5. Sidearm-assisted hydrogen activation.

Considering that a strong base in a stoichiometric amount is required under the optimized hydrogenation conditions, the existence of the protonated species $\mathbf{2H^+}$ is unlikely, ruling out pathway A.

DFT calculations of pathway C (Figure 3) revealed a reasonably stable carbamate-like intermediate **A**, followed by a reaction barrier of 31.7 kcal·mol^{-1} (**TS_AB**) toward forming the Ir-formate intermediate (**B**). On the other hand, when the direct hydride transfer to CO_2 was estimated, the reaction barrier dropped to 26.5 kcal·mol^{-1} (**TS_2B**), making this pathway favorable and in reasonable agreement with the reaction conditions.

10.1002/chem.202301915

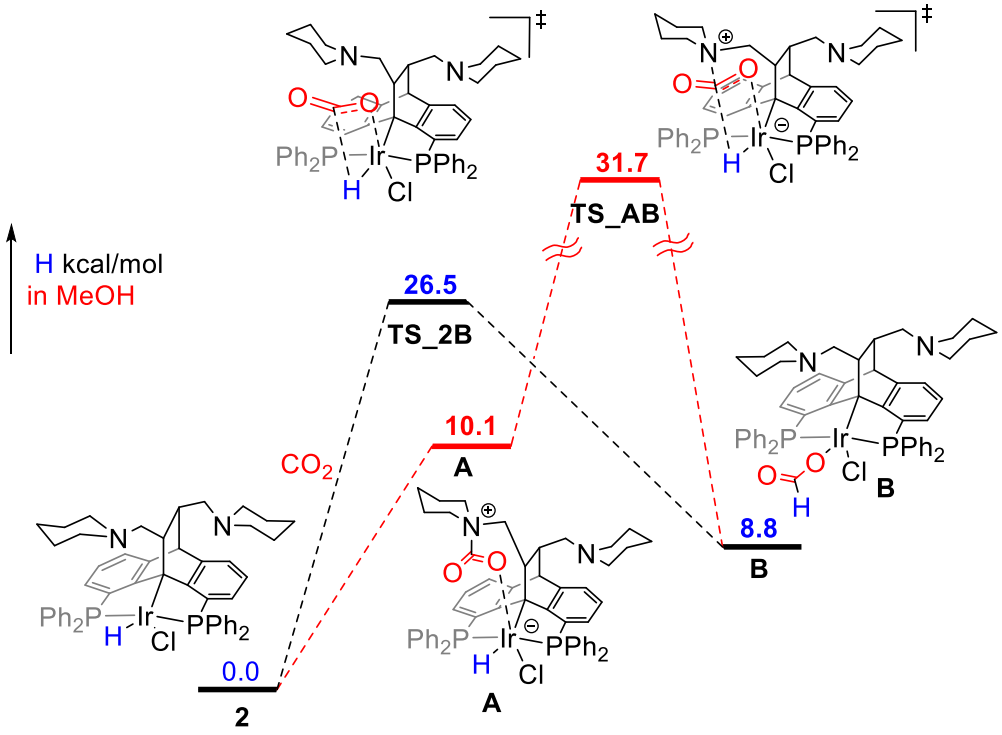

Figure 3. Computed reaction profiles for the ligand-assisted CO_2 activation (red) and direct hydride transfer (black) toward the hydride transfer step.

The mechanism underlying the heterolytic hydrogen activation by the bifunctional catalyst studied in our group often relies on non-oxidative heterolytic H-H bond splitting by a Lewis acidic metal and a basic ligand site (Scheme 6).

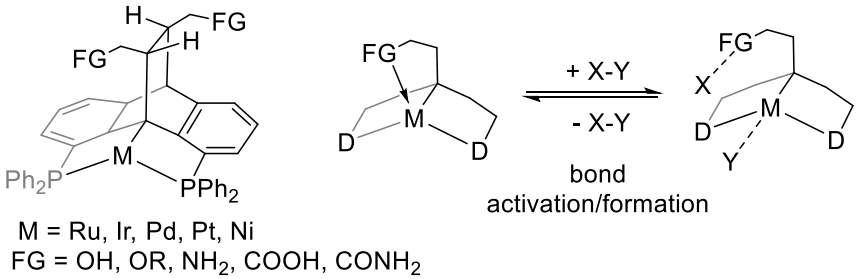

Scheme 6. Non-oxidative heterolytic bond activation via an MLC mechanism in 3-D pincer complexes.

10.1002/chem.202301915

Although analogous H_2 splitting by the amine-functionalized iridium(III) complexes such as **1** or **2** has not been studied yet, we hypothesize that Ir-H species are regenerated via the exact same non-oxidative mechanism. To probe this process, we exposed **2** to an excess of ammonium formate in THF/methanol, assuming protonolysis of the Ir–H bond to the corresponding formate species B (Scheme 5). Unfortunately, quick decomposition of the formate occurred under H_2-free conditions. Nevertheless, replacing ammonium formate with ammonium chloride resulted in a quick disappearance of the hydride peak and a lower-field shift of the phosphine signals (Scheme 7). When the product of this reaction,[32] structurally similar to the **B**, was pressurized with H_2 in THF, the hydride signals characteristic of **2** reappeared after three days at room temperature.[33]

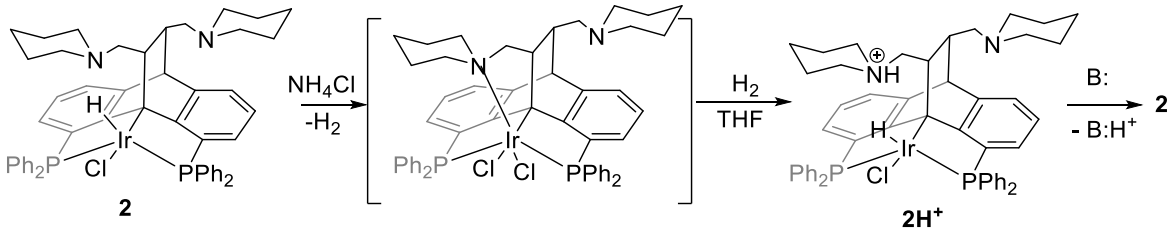

Scheme 7. Sidearm-assisted hydrogen activation.

DFT calculations complemented the *in situ* NMR experiment to get an insight into the mechanism of hydrogen activation by a hypothetical Ir-OOCH intermediate (**B**) and identify the reasonable pathway for the regeneration of **2** in the catalytic cycle (Figure 4). The computations suggested that the first step in this sequence may start with H_2 coordination to the 16-electron **B** (a 4 kcal·mol^{-1} uphill process leading to the formation of **B-H₂**). The polarization of coordinated H_2 facilitates the subsequent attack by the basic piperidine sidearm and heterolytic splitting via essentially barrier-less transition state (**TS_BC**) with respect to the **B-H₂** and only 4.1 kcal

10.1002/chem.202301915

kcal·mol^{-1} above **B**. The calculated reaction barrier correlates well with the room temperature conditions in the hydrogen activation experiment, implying that CO_2 hydrogenation is the bottleneck step.[34] Despite the zwitterionic nature of the intermediate **C**, this step is thermodynamically favorable (- 18.4 kcal·mol^{-1}). Still, the system can be further stabilized via base-assisted regeneration of **2** via formic acid elimination in the form of DBU-formate adduct.

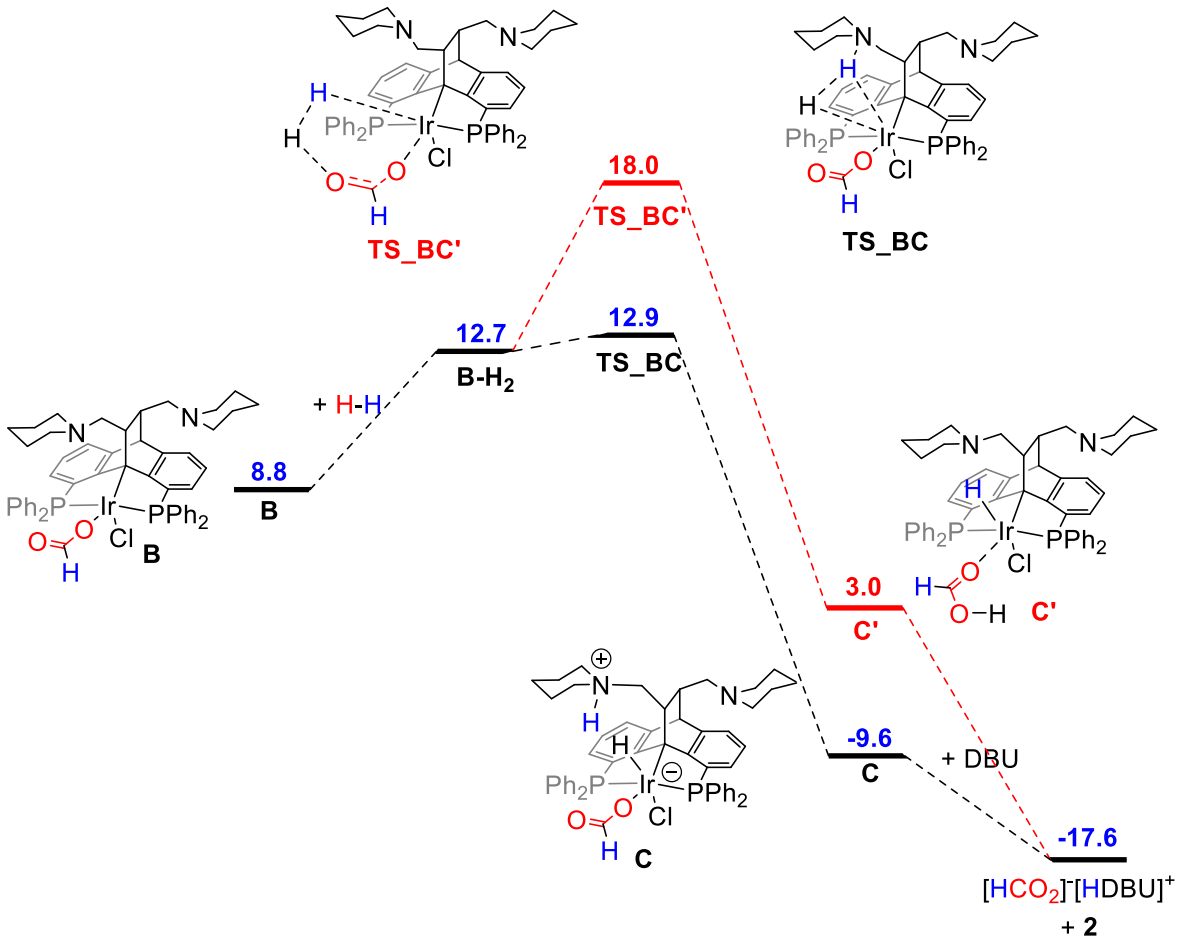

Figure 4. Computed reaction profiles for the ligand-assisted (black) and non-cooperative (red) H_2 activation by **B**.

Since we hold only indirect evidence for the tertiary amine sidearm participation in the reaction, we assessed computationally an alternative pathway where the heterolytic H_2 splitting occurs via metathetical reorganization (Figure 4, red). However, the corresponding **TS_BC'** was located at 5.1 kcal·mol^{-1} above **TS_BC** which makes this pathway less favoured.

Conclusions

In conclusion, we have described a highly efficient Ir catalyst for the selective hydrogenation of CO_2 to formic acid, demonstrating impressive performance (TON up to $6 \cdot 10^4$ and TOF up to $1.7 \cdot 10^4$ h^{-1}). The design of the bifunctional catalyst relies on a tertiary amine moiety in the secondary coordination sphere. Our experimental studies and quantum chemical calculations elaborated on the role of the pendant functional group. First, we demonstrated the heterolytic hydrogen activation via intramolecular deprotonation of the pre-coordinated H_2 molecule by the tertiary amine. Second, we suggested that the less coordinating nature of the amine with bulkier substituents facilitates the hydrogenation step. Nevertheless, the most important ramification of this work is that the unique topology of this family of compounds and flexibility in their synthesis offer essentially unlimited opportunities for the fine-tuning of the catalytic activity in many classical reaction schemes, as well as render new reactivity to many classical organometallic catalysts. Further mechanistic and catalytic studies are underway.

10.1002/chem.202301915

ASSOCIATED CONTENT

Experimental section

Complex 2 The complex was synthesized according to an adapted procedure. Di tert-Amine ligand (**3**) (0.903 mmol) and 0.5 eq of $[IrCl(COE)_2]_2$ (0.451 mmol) were stirred in a 1:1 mixture of IPA/ACN at RT for 8h. The solvents were evaporated, and the desired product was recrystallized from minimal amounts of cold methanol and diethyl ether. ^{1}H-NMR (THF-d_8), δ (ppm): -9.87 (dd, 1H, J_1(H-P) = 32.8 Hz, J2(H-P) = 152 Hz), 0.95-1.02 (m, 1H), 1.18-1.54 (m, 12H), 1.83-1.97 (m, 3H), 2.18-2.26 (m, 5H), 2.37 (s, 1H), 2.86-2.88 (m, 2H), 3.33-3.36 (m, 1H), 4.02 (t, 1H, J = 13.3 Hz), 4.28 (s, 1H), 6.11 (dd, 2H, J1 = 7.7 Hz, J2 = 11 Hz), 6.31 (dt, 2H, J1 = 2.3 Hz, J2 = 7.7 Hz), 6.54-6.61 (m, 3H), 6.72 (tq, 1H, J1 = 1.3 Hz, J2 = 7.5 Hz), 6.87 (dt, 1H, J1 = 3 Hz, J2 = 7.5 Hz), 6.97, (dt, 1H, J1 = 0.8 Hz, J2 = 7.5 Hz), 7.03-7.13 (m, 4H), 7.16 (dt, 1H, J1 = 1.7 Hz, J2 = 7.5 Hz), 7.21-7.24 (m, 4H), 7.41-7.49 (m, 3H), 7.75 (bs, 2H), 8.19-8.25 (m, 2H). 31PNMR (THF-d8), δ (ppm): 3.8 (1P) 14.34 (1P). 31PNMR (C2D2Cl4) decoupled from aromatics, δ (ppm): 4.76 (d, 1P, J = 70 Hz) 14.94 (d 1P, J = 365 Hz). Calcd for [M+H]+ 996.3080, found 996.3061.

Hydrogenation of CO_2 At catalyst load of 0.001mol% DBU (1.886 mmol) and **2** ($1.886*10^{-5}$ mmol) at a ratio of 100000/1 respectively were charged in a parr bomb apparatus. The apparatus was pressured with CO_2 and H_2. The parr bomb was set at the relevant temperature with stirring. At the end of the reaction, the parr bomb was cooled, the pressure was released, and the conversion was measured via NMR with DMF as standard (0.1 ml). 1HNMR of formate (DMSO-d6), δ (ppm): 9.022 (s, 1H). 1HNMR of methyl formate (DMSO-d6), δ (ppm): 8.572 (q4, 1H, J = 0.8 Hz), 4.182 ppm (d, 3H, J = 0.8 Hz) .

Computational details

Computational Studies. The calculations were performed using the Gaussian 09 program[35] employing B3PW91[36]-[37] functional and a standard split valence basis set def2-SVP.[38] The solvent effects, in our case for methanol, were taken into account during all the calculations by means of the SMD model.[39] All stationary points were fully characterized via analytical frequency calculations as either true minima (all positive eigenvalues) or transition states (one imaginary eigenvalue). The IRC procedure confirmed the nature of each transition state connecting two minima.[40] Zero-point vibrational energy corrections (ZPVE) were estimated by a frequency calculation at the same level of theory, to be considered for the calculation of the total energy values at T = 298 K.

Supporting Information. The Supporting Information is available free of charge at xxxx. The authors have cited additional references within the supporting information. [41]

The detailed synthesis of starting material, general procedures, characterization data, NMR spectra for all compounds, and cartesian coordinates. The crystallographic data was deposited to CCDC (2283154 and 2269254).

AUTHOR INFORMATION

Corresponding Authors

Prof. Dmitri Gelman - *dmitri.gelman@mail.huji.ac.il*.

Prof. Dr. Evamarie Hey-Hawkins – *hey@uni-leipzig.de*

Prof. Evgueni Kirillov - *evgueni.kirillov@univ-rennes1.fr*

Funding Sources

This research was supported by GIF (German-Israeli Foundation for Research and Development) Grant N I-1508-302.5/2019 and by the ISF (Israel Science Foundation) Grant No. 370/20. DG thanks Esther K. and M. Mark Watkins Chair for Synthetic Organic Chemistry. EK thanks ENSCR and the CTI group of ISCR for computational facilities. SGT thanks Prof. Dr. Evamarie Hey-Hawkins for the opportunity to carry out a part of the project at Leipzig University.

Notes

The authors declare no competing financial interest.

References

[1] B. Obama, *Science* **2017**, *355*, 126-129.

[2] a) S. A. Fors, C. A. Malapit, *ACS Catal.* **2023**, *13*, 4231-4249; b) J. Vaitla, Y. Guttormsen, J. K. Mannisto, A. Nova, T. Repo, A. Bayer, K. H. Hopmann, *ACS Catal.* **2017**, *7*, 7231-7244; c) M. D. Burkart, N. Hazari, C. L. Tway, E. L. Zeitler, *ACS Catal.* **2019**, *9*, 7937-7956; d) Y. Liu, X.-B. Lu, *Macromolecules* **2023**, *56*, 1759-1777; e) Y. Li, X. Cui, K. Dong, K. Junge, M. Beller, *ACS Catal.* **2017**, *7*, 1077-1086.

[3] R. R. Shaikh, S. Pornpraprom, V. D'Elia, *ACS Catal.* **2018**, *8*, 419-450.

[4] a) C. A. L. Lidston, S. M. Severson, B. A. Abel, G. W. Coates, *ACS Catal.* **2022**, *12*, 11037-11070; b) A. Centeno-Pedrazo, J. Perez-Arce, Z. Freixa, P. Ortiz, E. J. Garcia-Suarez, *Ind. Eng. Chem. Res.* **2023**, *62*, 3428-3443.

[5] X. Xiang, L. Guo, X. Wu, X. Ma, Y. Xia, *Env. Chem. Lett.* **2012**, *10*, 295-300.

[6] a) A. S. Lindsey, H. Jeskey, *Chem. Rev.* **1957**, *57*, 583-620; b) O. Mohammad, J. A. Onwudili, Q. Yuan, *RSC Sustain.* **2023**.

[7] a) P. G. Jessop, F. Joó, C.-C. Tai, *Coord. Chem. Rev.* **2004**, *248*, 2425-2442; b) W. Leitner, *Angew. Chem., Int. Ed.* **1995**, *34*, 2207-2221; c) Z. Hua, Y. Yang, J. Liu, *Coord. Chem. Rev.* **2023**, *478*, 214982; d) E. Furimsky, *Ind. Eng. Chem. Res.* **2020**, *59*, 15393-15423; e) C.-f. Li, R.-t. Guo, Z.-r. Zhang, T. Wu, W.-g. Pan, *Small* **2023**, *n/a*, 2207875.

[8] A. M. Klibanov, B. N. Alberti, S. E. Zale, *Biotech. Bioeng.* **1982**, *24*, 25-36.

[9] a) P. Kalck, C. Le Berre, P. Serp, *Coord. Chem. Rev.* **2020**, *402*, 213078; b) A. Haynes, in *Adv. Catal., Vol. 53* (Eds.: B. C. Gates, H. Knözinger), Academic Press, **2010**, pp. 1-45.

[10] a) V. M. Ramos, A. G. S. de Oliveira-Filho, A. P. de Lima Batista, *J. Phys. Chem. A* **2022**, *126*, 2082-2090; b) S. Kar, A. Goeppert, J. Kothandaraman, G. K. S. Prakash, *ACS Catalysis* **2017**, *7*, 6347-6351; c) Y. Zhang, A. D. MacIntosh, J. L. Wong, E. A. Bielinski, P. G. Williard, B. Q. Mercado, N. Hazari, W. H. Bernskoetter, *Chem. Sci.* **2015**, *6*, 4291-4299; d) F. Bertini, N. Gorgas, B. Stoger, M. Peruzzini, L. F. Veiros, K. Kirchner, L. Gonsalvi, *ACS Catal.* **2016**, *6*, 2889-2893; e) J. Schneidewind, R. Adam, W. Baumann, R. Jackstell, M. Beller, *Angew. Chem. Int. Engl. Ed.* **2017**, *56*, 1890-1893; f) V. Zubar, Y. Lebedev, L. M. Azofra, L. Cavallo, O. El-Sepelgy, M. Rueping, *Angew. Chem. Int. Engl. Ed.* **2018**, *57*, 13439-13443; g) F. Bertini, M. Glatz, N. Gorgas, B. Stöger, M. Peruzzini, L.

F. Veiros, K. Kirchner, L. Gonsalvi, *Chem. Sci.* **2017**, *8*, 5024-5029; h) S. Kostera, S. Weber, M. Peruzzini, L. F. Veiros, K. Kirchner, L. Gonsalvi, *Organometallics* **2021**, *40*, 1213-1220; i) L. Gonsalvi, A. Guerriero, S. Kostera, in *CO2 Hydrogenation Catalysis*, **2021**, pp. 53-88; j) K. Schlenker, E. G. Christensen, A. A. Zhanserkeev, G. R. McDonald, E. L. Yang, K. T. Lutz, R. P. Steele, R. T. VanderLinden, C. T. Saouma, *ACS Catal.* **2021**, *11*, 8358-8369.

[11] a) R. Tanaka, M. Yamashita, K. Nozaki, *J. Am. Chem. Soc.* **2009**, *131*, 14168-14169; b) T. J. Schmeier, G. E. Dobereiner, R. H. Crabtree, N. Hazari, *J. Am. Chem. Soc.* **2011**, *133*, 9274-9277; c) S. Kar, R. Sen, J. Kothandaraman, A. Goeppert, R. Chowdhury, S. B. Munoz, R. Haiges, G. K. S. Prakash, *J. Am. Chem. Soc.* **2019**, *141*, 3160-3170; d) S.-T. Bai, G. De Smet, Y. Liao, R. Sun, C. Zhou, M. Beller, B. U. W. Maes, B. F. Sels, *Chem. Soc. Rev.* **2021**, *50*, 4259-4298; e) K.-I. Tominaga, Y. Sasaki, M. Saito, K. Hagihara, T. Watanabe, *J. Mol. Cat.* **1994**, *89*, 51-55; f) C. A. Huff, M. S. Sanford, *J. Am. Chem. Soc.* **2011**, *133*, 18122-18125; g) P. Munshi, A. D. Main, J. C. Linehan, C.-C. Tai, P. G. Jessop, *J. Am. Chem. Soc.* **2002**, *124*, 7963-7971; h) E. Balaraman, C. Gunanathan, J. Zhang, L. J. W. Shimon, D. Milstein, *Nat. Chem.* **2011**, *3*, 609-614; i) S. Wesselbaum, T. vom Stein, J. Klankermayer, W. Leitner, *Angew. Chem. Int. Engl. Ed.* **2012**, *51*, 7499-7502; j) M. Czaun, A. Goeppert, J. Kothandaraman, R. B. May, R. Haiges, G. K. S. Prakash, G. A. Olah, *ACS Catal.* **2014**, *4*, 311-320; k) S. Moret, P. J. Dyson, G. Laurenczy, *Nat. Commun.* **2014**, *5*, 4017; l) A. M. Lilio, M. H. Reineke, C. E. Moore, A. L. Rheingold, M. K. Takase, C. P. Kubiak, *J. Am. Chem. Soc.* **2015**, *137*, 8251-8260; m) N. M. Rezayee, C. A. Huff, M. S. Sanford, *J. Am. Chem. Soc.* **2015**, *137*, 1028-1031; n) L. Wang, N. Onishi, K. Murata, T. Hirose, J. T. Muckerman, E. Fujita, Y. Himeda, *ChemSusChem* **2017**, Ahead of Print; o)

Z. Wang, Z. Zhao, Y. Li, Y. Zhong, Q. Zhang, Q. Liu, G. A. Solan, Y. Ma, W.-H. Sun, *Chem. Sci.* **2020**, *11*, 6766-6774; p) R. Sen, A. Goeppert, G. K. Surya Prakash, *Angew. Chem. Int. Engl. Ed.* **2022**, *61*, e202207278.

[12] a) C. Mealli, R. Hoffmann, A. Stockis, *Inorg. Chem.* **1984**, *23*, 56-65; b) W. Leitner, *Coord. Chem. Rev.* **1996**, *153*, 257-284.

[13] a) C. S. Yeung, V. M. Dong, *J. Am. Chem. Soc.* **2008**, *130*, 7826-7827; b) R.-Z. Zhang, B.-Y. Wu, Q. Li, L.-L. Lu, W. Shi, P. Cheng, *Coord. Chem. Rev.* **2020**, *422*, 213436.

[14] a) D. J. Evans, C. J. Pickett, *Chem. Soc. Rev.* **2003**, *32*, 268-275; b) D. J. Evans, *Coord. Chem. Rev.* **2005**, *249*, 1582-1595; c) M. Can, F. A. Armstrong, S. W. Ragsdale, *Chem. Rev.* **2014**, *114*, 4149-4174.

[15] a) R. Puerta-Oteo, M. Holscher, M. V. Jimenez, W. Leitner, V. Passarelli, J. J. Perez-Torrente, *Organometallics* **2018**, *37*, 684-696; b) W. H. Bernskoetter, N. Hazari, *Acc. Chem. Res.* **2017**, *50*, 1049-1058; c) E. Fujita, J. T. Muckerman, Y. Himeda, *Biochim. Biophys. Acta, Bioenerg.* **2013**, *1827*, 1031-1038; d) S. Sung, D. Kumar, M. Gil-Sepulcre, M. Nippe, *J. Am. Chem. Soc.* **2017**, *139*, 13993-13996; e) E. Haviv, D. Azaiza-Dabbah, R. Carmieli, L. Avram, J. M. L. Martin, R. Neumann, *J. Am. Chem. Soc.* **2018**, *140*, 12451-12456; f) C. Costentin, S. Drouet, M. Robert, J.-M. Saveant, *Science* **2012**, *338*, 90-94; g) C. Costentin, G. Passard, M. Robert, J.-M. Saveant, *J. Am. Chem. Soc.* **2014**, *136*, 11821-11829; h) A. Chapovetsky, T. H. Do, R. Haiges, M. K. Takase, S. C. Marinescu, *J. Am. Chem. Soc.* **2016**, *138*, 5765-5768; i) K. T. Ngo, M. McKinnon, B. Mahanti, R. Narayanan, D. C. Grills, M. Z. Ertem, J. Rochford, *J. Am. Chem. Soc.* **2017**, *139*, 2604-2618; j) A. Noor, S. Qayyum, T. Bauer, S. Schwarz, B. Weber, R. Kempe, *Chem. Commun.* **2014**, *50*, 13127-13130.

[16] a) D. Gelman, S. Musa, *ACS Catal.* **2012**, *2*, 2456-2466; b) A. Singh, D. Gelman, *ACS Catal.* **2020**, *10*, 1246-1255; c) S. De-Botton, D. S. O. A. Filippov, E. S. Shubina, N. V. Belkova, D. Gelman, *ChemCatChem* **2020**, *12*, 5959-5965; d) C. Shirel, A. N. Bilyachenko, D. Gelman, *Eur. J. Inorg. Chem.* **2019**; e) V. A. Kirkina, G. A. Silantyev, S. De-Botton, O. A. Filippov, E. M. Titova, A. A. Pavlov, N. V. Belkova, L. M. Epstein, D. Gelman, E. S. Shubina, *Inorg. Chem.* **2020**, *59*, 11962-11975; f) D. Gelman, R. Romm, *Top. Organomet. Chem.* **2013**, *40*, 289-318.

[17] a) S. Cohen, V. Borin, I. Schapiro, S. Musa, S. De-Botton, N. V. Belkova, D. Gelman, *ACS Catal.* **2017**, *7*, 8139-8146; b) S. Mujahed, F. Valentini, S. Cohen, L. Vaccaro, D. Gelman, *ChemSusChem* **2019**, *12*, 4693-4699; c) S. Mujahed, E. Hey-Hawkins, D. Gelman, *Chem.-Eur. J.* **2022**, e202201098; d) S. Mujahed, M. S. Richter, E. Kirillov, E. Hey-Hawkins, D. Gelman, *Isr. J. Chem.* **2023,** e202300037.

[18] S. Tshepelevitsh, A. Kütt, M. Lõkov, I. Kaljurand, J. Saame, A. Heering, P. G. Plieger, R. Vianello, I. Leito, *Eur. J. Org. Chem.* **2019**, *2019*, 6735-6748.

[19] T. Kanzian, T. A. Nigst, A. Maier, S. Pichl, H. Mayr, *Eur. J. Org. Chem.* **2009**, *2009*, 6379-6385.

[20] a) C. Azerraf, A. Shpruhman, D. Gelman, *Chem. Commun.* **2009**, 466-468; b) S. De-Botton, R. Romm, G. Bensoussan, M. Hitrik, S. Musa, D. Gelman, *Dalton Trans.* **2016**, *45*, 16040-16046; c) S. Musa, A. Shpruhman, D. Gelman, *J. Organomet. Chem.* **2012**, *699*, 92-95; d) H. Schumann, O. Stenzel, S. Dechert, F. Girgsdies, J. Blum, D. Gelman, R. L. Halterman, *Eur. J. Inorg. Chem.* **2002**, 211-219.

[21] a) C. Azerraf, S. Cohen, D. Gelman, *Inorg. Chem.* **2006**, *45*, 7010-7017; b) L. Kaganovsky, K.-B. Cho, D. Gelman, *Organometallics* **2008**, *27*, 5139-5145; c) L. Kaganovsky, D.

Gelman, K. Rueck-Braun, *J. Organomet. Chem.* **2009**, *695*, 260-266; d) I. Kisets, D. Gelman, *Organometallics* **2018**, *37*, 526-529.

[22] a) S. Musa, O. A. Filippov, N. V. Belkova, E. S. Shubina, G. A. Silantyev, L. Ackermann, D. Gelman, *Chem. Eur. J.* **2013**, *19*, 16906-16909; b) Y. Radchenko, S. Mujahed, S. Musa, D. Gelman, *Inorg. Chim. Acta* **2021**, *521*, 120350.

[23] P. G. Jessop, T. Ikariya, R. Noyori, *Chem. Rev.* **1995**, *95*, 259-272.

[24] The use the expensive additive is not ideal. However, DBU can be recovered and reused.

[25] D. J. Heldebrant, P. G. Jessop, C. A. Thomas, C. A. Eckert, C. L. Liotta, *J. Org. Chem.* **2005**, *70*, 5335-5338.

[26] a) L. Zhang, M. Pu, M. Lei, *Dalton Trans.* **2021**, *50*, 7348-7355; b) Y. Matsubara, D. C. Grills, Y. Koide, *Chem. Lett.* **2019**, *48*, 627-629.

[27] Control experiments utilizing functionless PC(sp^3)P pincer iridium(III) catalysts led to significantly lower reactivity (SI).

[28] a) N. Makuve, G. Mehlana, R. Tia, J. Darkwa, B. C. E. Makhubela, *J. Organomet. Chem.* **2019**, *899*, 120892; b) H.-K. Lo, C. Copéret, *ChemCatChem* **2019**, *11*, 430-434; c) S. Oldenhof, J. I. van der Vlugt, J. N. H. Reek, *Catal. Sci. Technol.* **2016**, *6*, 404-408.

[29] G. A. Filonenko, R. van Putten, E. N. Schulpen, E. J. M. Hensen, E. A. Pidko, *ChemCatChem* **2014**, *6*, 1526-1530.

[30] N. Bothra, S. Das, S. K. Pati, *Chem. - Eur. J.* **2021**, *27*, 16407-16414.

[31] a) G. H. Lorimer, M. R. Badger, T. J. Andrews, *Biochem.* **1976**, *15*, 529-536; bC. Bathellier, L. J. Yu, G. D. Farquhar, M. L. Coote, G. H. Lorimer, G. Tcherkez, *Proc. Natl. Acad. Sci. USA* **2020**, *117*, 24234-24242.

[32] Deposition Numbers <url href="https://www.ccdc.cam.ac.uk/services/structures?id=doi:10.1002/chem.20230XXX"> 22695524 (for complex 2), 2283154 (for stas8 in SI), </url> contain the supplementary crystallographic data for this paper. These data are provided free of charge by the joint Cambridge Crystallographic Data Centre and Fachinformationszentrum Karlsruhe <url href="http://www.ccdc.cam.ac.uk/structures">Access Structures service</url>.

[33] The free ligand was not detected under these conditions indicating the stability of the metal-carbon bond in our PC(sp^3)P pincer complexes under hydrogenative conditions.

[34] The clear dependence of the hydrogenation rate on the partial pressure of CO_2 supports this assumption (Table 2, entries 9-11)

[35] M. J., Frisch, G. W. Trucks, H. B. Schlegel, G. E. Scuseria, M. A. Robb, J. R. Cheeseman, G. Scalmani, V. Barone, B. Mennucci, G. A. Petersson, H. Nakatsuji, M. Caricato, X. Li, H. P. Hratchian, A. F. Izmaylov, J. Bloino, G. Zheng, J. L. Sonnenberg, M. Hada, M. Ehara, K. Toyota, R. Fukuda, J. Hasegawa, M. Ishida, T. Nakajima, Y. Honda, O. Kitao, H. Nakai, T. Vreven, J. A. Montgomery Jr., J. E. Peralta, F. Ogliaro, M. Bearpark, J. J. Heyd, E. Brothers, K. N. Kudin, V. N. Staroverov, R. Kobayashi, J. Normand, K. Raghavachari, A. Rendell, J. C. Burant, S.S Iyengar, J. Tomasi, M. Cossi, N. Rega, J.M. Millam, M. Klene, J. E. Knox, J. B. Cross, V. Bakken, C. Adamo, J. Jaramillo, R. Gomperts, R. E. Stratmann, O. Yazyev, A. J. Austin, A. J, R. Cammi, C. Pomelli, J. W. Ochterski, R. L. Martin, K. Morokuma, V. G. Zakrzewski, G. A. Voth, P. Salvador, J. J. Dannenberg, S. Dapprich, A. D. Daniels, Ö. Farkas, J. B. Foresman, J. V. Ortiz, J. Cioslowski, D. J. Fox, Gaussian 09, Revision D.01; Gaussian Inc.: Pittsburgh, PA, **2009**.

[36] A.D. Becke, . *Phys. Rev. A* **1988**, *38*, 3098–3100.

[37] A.D. Becke, J. *Chem. Phys.* **1993**, *98*, 5648–5652.

[38] F. Weigend, R. Ahlrichs, *Phys. Chem. Chem. Phys*. **2005**, *7*, 3297-305.

[39] A. V. Marenich, C. J. Cramer, D. G. Truhlar, *J. Phys. Chem. B*, **2009**, *113*, 6378–6396.

[40] C. Gonzales, H.B. Schlegel, *J. Chem. Phys*. **1989**, *90*, 2154–2161.

[41] a) O. Grossman, C. Azerraf, D. Gelman, *Organometallics* **2006**, *25*, 375-381; b) D. Bézier, M. Brookhart, *ACS Catal.* **2014**, *4*, 3411-3420.

ToC

Hydrogenation of CO_2 under molecular hydrogen by a fully characterized Ir(III) pincer complex is described. The unique biomimetic second coordination sphere functionality is investigated both empirically and computationally shows the hydrogen activation step to proceed in room temperature.

10.1002/chem.202301915

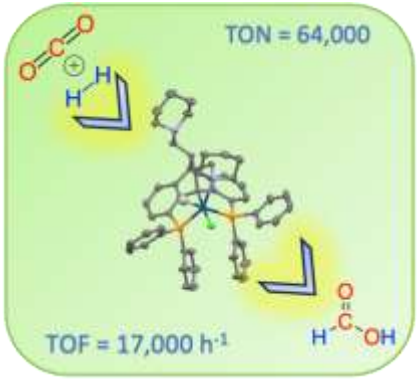

Twitter handles:

Gelman Group - @GelmanGroup

Stanislav Gelman Tropp - @Stas_Wild

Prof. Dr. Evamarie Hey-Hawkins - @HeyHawkins